

POSSIBILITIES AND FUNDAMENTAL LIMITATIONS OF POSITIONING USING WIRELESS COMMUNICATION NETWORKS MEASUREMENTS

Fredrik Gustafsson and Fredrik Gunnarsson*,***

*Department of Electrical Engineering
Linköping University, SE-581 83 Linköping, Sweden
Email: fredrik@isy.liu.se, fred@isy.liu.se
**Ericsson Research, Linköping, Sweden

ABSTRACT

Positioning in wireless networks is today mainly used for yellow page services, but its importance will grow when emergency call services become mandatory and with the advent of more advanced location based services and mobile gaming. It is also plausible that future resource management algorithms may rely on position estimation and prediction. We will in this survey paper discuss and illustrate possibilities and fundamental limitations associated with mobile positioning.

1. INTRODUCTION

Various location-based services in wireless communication networks depend on mobile positioning. Commercial examples range from low-accuracy methods based on cell identity identification to high-accuracy methods combining wireless network information and satellite positioning. These methods are typically *network-centric*, where the position is determined in the network and presented to the user via a specific service. Due to logistic reasons, the position is estimated from *static snapshot measurements* possibly provided by the *mobile station (MS)*. *Mobile-centric* solutions enable the use of *sampled temporal measurements* and *motion models* to enhance estimation accuracy and integrity. Measurements either explicitly or implicitly relate the MS position to the position of *reference points (RP)* (e.g. positions of radio base stations or satellites), or to the specific behavior of the MS and

This work is supported by the competence center ISIS (Information Systems for Industrial Control and Supervision), and in cooperation with Ericsson Research.

its surrounding environment. Measurements are typically directional, such as the *angle of arrival*, (AOA) between MS and RP, or related to relative distances, such as the *time of arrival* (TOA), *time difference of arrival* (TDOA) and *received signal strength* (RSS). The survey articles [1, 2, 3] provide further information about positioning in wireless networks and associated standardization. Indoor positioning is discussed in[4], which includes its own specific challenges.

While yellow pages services require only crude position estimates (such as cell identity), more advanced services like mobile gaming could benefit from accurate and timely position estimates. Furthermore, the emergency call accuracy requirements by the Federal Communications Commission (FCC), have been tightened recently [5] to 300 m for 95% of the calls and 100 m for 67% of the calls using network-centric methods, and 150 m and 50 m for 95% and 67% of the calls, respectively, using mobile-centric methods. Therefore, it is of interest to discuss achievable accuracies of the different methods.

This tutorial-oriented paper focuses on positioning based on uncertain measurements. In essence, position estimation is interpreted as a problem of solving systems of nonlinear equations. The accuracy of the solution is related to the information in the measurements through the Fisher Information Matrix. This provides a general basis for analyzing sensor configuration and sufficiency of information for specific accuracy requirements. The static case can be approached by either applying a stochastic gradient algorithm, or by numerically approximating the nonlinear least squares problem using Monte Carlo based techniques. The latter method can also be applied to the dynamic case with a motion model of the mobile, and is more generally applicable to various information, e.g. digital map information. The described methods apply to general wireless network measurements, but specific applications will be exemplified.

The outline is as follows: Section 2 discusses and models different measurements. Three archetypical measurements are used as illustration examples throughout the article: range measurements, range difference measurements and maps. Throughout the paper, a simplistic network example provides intuition, and a realistic deployment scenario is used to further illustrate the concepts. Section 3 discusses different ways to estimate position from one snapshot measurement. Focus is on the information provided by each measurement, which indicates achievable performance. Section 4 overviews different filtering approaches to make use of temporal correlation of the position, and rule of thumbs for how much the information is increased by filtering, are provided.

2. MEASUREMENTS

The observed measurements generate a set of nonlinear equations. With the general approach in this tutorial, it is straight-forward to introduce further measurements. This brief section exemplifies the measurements to illustrate

the ideas. Details regarding practical implementations and standards are adopted from [2, 3, 6, 7].

Denote the two-dimensional mobile position at time t by $p_t = (X_t, Y_t)^T$, and the known base station positions by $p^i = (X_i, Y_i)^T$. The generic measurements relative reference point i , y_t^i are subject to uncertainties e_t^i and typical measurements are summarized below. All measured times are automatically multiplied by the speed of light to get a measure in meters rather than in nano seconds.

- **Received signal strength:** $y_t^i = h_{RSS}(|p_t - p^i|) + e_t^i$ is averaged over fast fading, and depends on distance and slow fading. A model that solely depends on the relative distance is the so called Okumura-Hata model [8] $y_t^i = K - 10\alpha \log_{10}(|p_t - p^i|) + e_t^i$, where $\text{std}(e_t^i) \approx 4 - 12$ dB depending on the environment (desert to dense urban). It is also possible to utilize a predicted or measured spatial digital map with received signal strength values as discussed below.
- **Time of arrival:** $y_t^i = |p_t - p^i| + e_t^i = h_{TOA}(p_t, p^i) + e_t^i$ is for example estimated in the uplink in GSM at multiple base stations upon request from the network. It is also estimated from a multitude of satellites in the GPS (Global Positioning System). The 3G systems will feature assisted-GPS, where required information for measurement setup and positioning calculations are broadcasted in each cell by the base stations in the cellular network, which improves reliability and reduces time to position fix. Such measurements can also be seen as TOA measurements. The performance depends mainly on the synchronization accuracy, and GPS typically feature an accuracy in the order of 10 m in unobstructed environments.
- **Time difference of arrival:** $y_t^{i,j} = |p_t - p^i| - |p_t - p^j| + e_t^{i,j} = h_{TDOA}(p_t, p^i, p^j) + e_t^{i,j}$ is a practical mobile measurement related to relative distance. The measurements are reported to the network, which performs necessary computations and it is not necessary to communicate the network synchronization nor the reference point locations to the mobile. As for TOA, the synchronization accuracy determines the performance, but also the base station locations. The observed TDOA accuracy requirement for location purposes in WCDMA is 0.5 chip [2] which means an error of about 40 m ($\sigma_e \approx 20\text{m}$). Similarly, a TDOA accuracy requirement of 0.5 chip in cdma2000 (advanced forward link trilateration - A-FLT) means 120 m ($\sigma_e \approx 60\text{m}$) due to the lower chip rate. Satellite navigation systems feature even better accuracies.
- **Angle of arrival:** $y_t^i = h_{AOA}(p_t, p^i) + e_t^i$ is today mainly available as a very crude sector information (*e.g* 120°). With the use of group antennas this will be improved to about 30° beam width ($\sigma_e \approx 8$ degrees). and perhaps even better. Geometrically, the spatial resolution of the intersection of two perfectly complementing AOA measurements is limited to $2D \sin(\alpha/2)$, where α is the angular resolution and D the distance between the antennas. For $\alpha = 30^\circ$, this means 36% of D .

- **Digital map information:** $y_t = h_{MAP}(p_t, p^i) + e_t$ contains for instance RSS measurements relative the reference points either predicted or provided via dedicated measurement scans in the service area. The former is conducted in the network deployment phase using graphical information systems dedicated for network planning, like the TEMS CellPlanner Universal (<http://www.ericsson.com/tems/>) by Ericsson. The prediction grid is usually from 100 m down to a few meters when considering building data. Figure 1 illustrates such digital prediction maps. Performing actual measurements is only plausible in very limited service areas, like indoor. Most of the shadowing is included in the maps, and the remaining shadow fading component has typically $\text{std}(e_t^i) \approx 3$ dB depending on the environment and spatial map resolution. The map can also be a commercial street map for automotive terminals [9] as exemplified in Figure 1. A support to GPS for sea navigation was proposed in [10] using sonar depth measurements and a depth map.
- **Inertial sensors:** $y_t = h_{INS}(\dot{p}_t, \ddot{p}_t) + e_t$ describe the terminal movements relative a fixed coordinate system based on accelerometers, gyros, etc. Estimated Doppler frequencies also indicate relative velocities.
- **Position estimates:** from alternative sensors, such as a GPS receiver.

Received signal strength:	$y_t^i = h_{RSS}(p_t - p^i) + e_t^i$	4-12 dB (10 dB)
Time of arrival:	$y_t^i = p_t - p^i + e_t^i = h_{TOA}(p_t, p^i) + e_t^i$	5-100 m (14 m)
Time difference of arrival:	$y_t^{i,j} = p_t - p^i - p_t - p^j + e_t^{ij} = h_{TDOA}(p_t, p^i, p^j) + e_t^{ij}$	10-60 m (20 m)
Angle of arrival:	$y_t^i = h_{AOA}(p_t, p^i) + e_t^i$	$5^\circ - 10^\circ$ (6°)
Digital map information:	$y_t = h_{MAP}(p_t) + e_t$	(RSS map, 3 dB)
Inertial sensors:	$y_t = h_{INS}(\dot{p}_t, \ddot{p}_t) + e_t$	
Position estimates (e.g. GPS):	$y_t = p_t + e_t$	5-20 m

Table 1. Mathematical notation of available measurements in wireless communication systems together with approximative noise standard deviations σ_e . Here y is the actual numerical value, h denotes a general non-linear model, p_t is the sought position, p^i denotes the position of base station/antenna number i and e denotes measurement noise with a probability density function $p_E(\cdot)$. The noise standard deviation values in parantheses indicate values used in numerical evaluations, and represent a favorable situation with essentially line-of-sight measurements. Note that the quality of the sensor information depends not only on the the noise variance, but also on the size and variation in $h(p)$. This is discussed in Section 3.2.

Example 1 Consider the scenario in Figure 2, where four receivers are placed in the positions $(-1,0)$, $(1,0)$, $(0,-1)$ and $(0,1)$, respectively. Each receiver measures the arrival time of a transmitted signal from an unknown position,

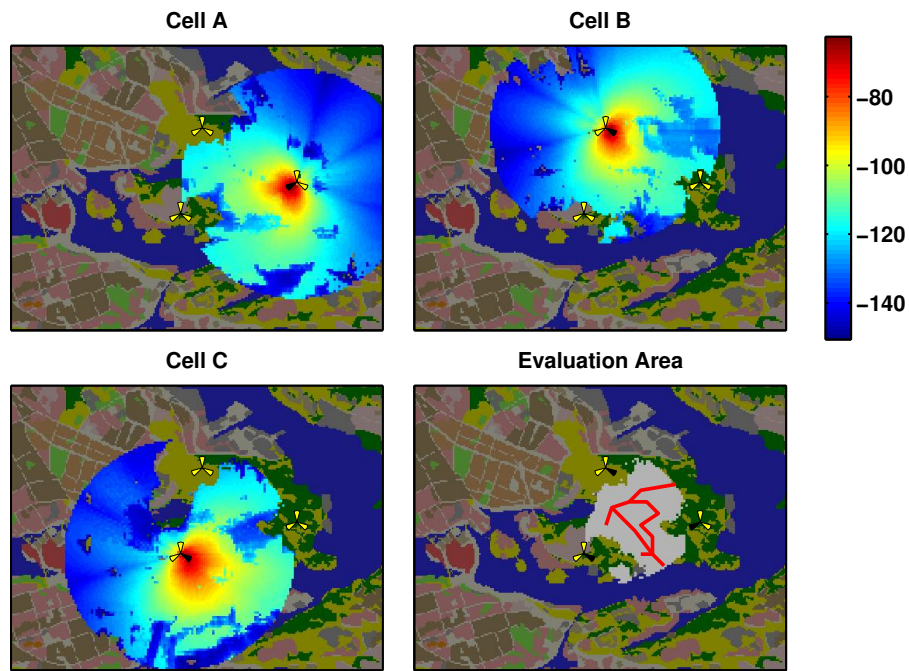


Fig. 1. Example of RSS predictions with the spatial resolution 40 m using TEMS CellPlanner Universal. The artificial network is deployed at Djurgården, Stockholm, Sweden (true terrain data, and fictitious but realistic base station locations). Predicted power gain from three cells A, B and C is roughly directed towards the interior area between the base station. The evaluation area used in examples is the shaded area in the last plot, where all three cells can be detected. A simple and artificial road map is also depicted.

using accurate and synchronized clocks. If the transmitter is also synchronized, the signal propagation time can be computed, which leads to a TOA measurement. Propagation time corresponds to a distance, which leads to the distance circles around each receiver in Figure 2. If the transmitter is unsynchronized, each pair of receivers can compute a time-difference of arrival TDOA. This leads to a hyperbolic function where the transmitter can be located [11]. Four receivers can compute six such hyperbolic functions, which intersect in one unique point, see Figure 2.

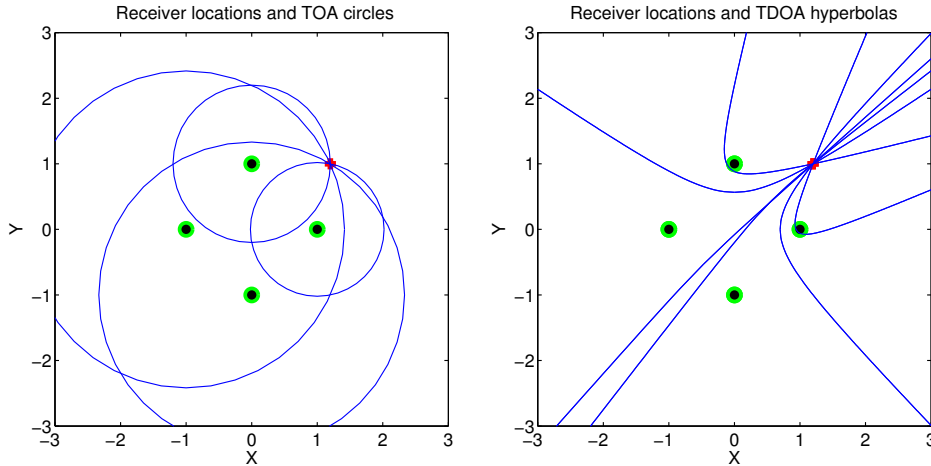


Fig. 2. Example scenario: four receivers are placed in a square, and there is one transmitter at (1.2,1). With TOA measurements, each receiver measurement constrains the transmitter position to a circle, while with TDOA measurements, each *pair of* receiver measurements constrain the transmitter position to a hyperbola.

3. STATIC CASE

In the static case, no assumption of temporal correlation of the position is done, so the position vector is a sequence of uncorrelated parameters estimated in a snap-shot manner. Knowledge of measurement error distributions can improve the performance, and Cramer-Rao lower bounds serve as fundamental performance limits.

3.1. Estimation Criteria

The static case provides snapshot measurements y of some quantities related to the position p . Suppose all measurements at time t are collected in the vector y_t related to the position by $y_t = h(p_t) + e_t$. The problem is thus to minimize $\|y_t - h(p)\|$ over p in some suitable norm. The most common choices of norms are summarized in Table 2.

Non-linear Least Squares	NLS	$V^{NLS}(p) = \ y_t - h(p)\ ^2 = (y_t - h(p))^T(y_t - h(p))$
Weighted Non-linear Least Squares	WNLS	$V^{WNLS}(p) = (y_t - h(p))^T R_t^{-1}(p)(y_t - h(p))$
Maximum Likelihood	ML	$V^{ML}(p) = \log p_E(y_t - h(p))$
Gaussian ML	GML	$V^{GML}(p) = (y_t - h(p))^T R_t^{-1}(p)(y_t - h(p)) + \log \det R_t(p)$

Table 2. Optimization criteria $V(p)$ for estimating position p from uncertain measurements $y = h(p) + e$ using $\hat{p}_t = \arg \min_p V(p)$.

Table 2 starts with the non-linear least squares criterion. In a stochastic setting where the measurements are subject to a stochastic unknown error e_t , optimizing the 2-norm is still the best thing to do if the errors are independent identically distributed (i.i.d) Gaussian variables, that is $e_t \in N(0, \sigma_e^2 I)$. If there is a spatial correlation, or if the measurements are of different quality over time or for different sensors, improvements are possible. In these cases where $\text{Cov}(e_t) = R_t$, the weighted NLS is to prefer. Further, with a given error probability distribution $p_E(e)$, the Maximum Likelihood (ML) approach provides an efficient estimator. In the special case with a Gaussian error distribution with position dependent covariance $e_t \in N(0, R(p_t))$, the ML criterion is similar to the WNLS criterion, but with the term $\log \det R_t(p)$. This prevents the selection of positions with large uncertainty (large $R(p_t)$), which could be the case with WNLS.

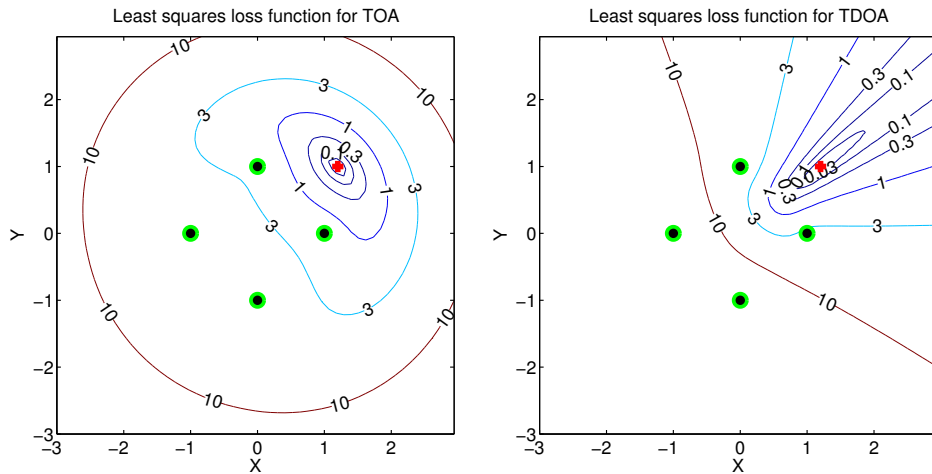


Fig. 3. Least squares (negative log likelihood) loss functions for TOA and TDOA measurements, respectively in the scenario in Example 1.

Example 2 Figure 3 shows the NLS loss functions corresponding to the scenario in Example 1.

3.2. Fundamental Performance Bounds

The *Fisher Information Matrix (FIM)* provides a fundamental estimation limit referred to as the *Cramer-Rao Lower Bound (CRLB)* [12]. This bound has been analyzed thoroughly in the literature, primarily for AOA, TOA and TDOA [13, 14, 15, 16, 17, 18, 19, 20], but also for RSS [21, 22] and with specific attention to the impact from non-line-of-sight [23, 24].

The Fisher Information Matrix $J(p)$ is defined as

$$\begin{aligned} J(p) &= \mathbb{E} \left(\frac{d \log p_E(y - h(p))}{d p} \right)^T \frac{d \log p_E(y - h(p))}{d p} \\ &= \mathbb{E} \left(\begin{array}{cc} \left(\frac{d \log p_E(y - h(X, Y))}{d X} \right)^2 & \frac{d \log p_E(y - h(X, Y))}{d X} \frac{d \log p_E(y - h(X, Y))}{d Y} \\ \frac{d p_E(y - h(X, Y))}{d X} \frac{d \log p_E(y - h(X, Y))}{d Y} & \left(\frac{d p_E(y - h(X, Y))}{d Y} \right)^2 \end{array} \right) \end{aligned} \quad (1)$$

In case of Gaussian measurement errors $e \sim \mathcal{N}(0, R(p))$, FIM equals

$$J(p) = H^T(p) R(p)^{-1} H(p), \quad (2)$$

$$H(p) = \frac{d h(p)}{d p} = \left(\frac{d h(X, Y)}{d X}, \frac{d h(X, Y)}{d Y} \right). \quad (3)$$

The larger gradient $H(p)$, or the smaller measurement error, the more information is provided from the measurement, and the smaller potential estimation error.

Information is additive, so if two measurements are independent, the corresponding information matrices can be added. This is easily seen for instance from (2) for $H^T = (H_1^T, H_2^T)$ and R being block diagonal, in which case we can write $J = J_1 + J_2$. Plausible approximative scalar information measures are the trace of the FIM and the smallest eigenvalue of FIM

$$J_{\text{tr}}(p) \triangleq \text{tr } J(p), \quad J_{\text{min}}(p) \triangleq \min \text{eig } J(p). \quad (4)$$

The former information measure is additive as FIM itself, while the latter is an under-estimation of the information useful when reasoning about whether the available information is sufficient or not. Note that in the Gaussian case with a diagonal measurement error covariance matrix, the trace of FIM is the squared gradient magnitude. Figure 4 illustrates the information in the typical measurements in the artificial network from Figure 1 using the error standard deviations from Table 1. It is evident that RSS is the least informative, then AOA, and TOA/TDOA the most informative. The RSS map increases the information level to the same as AOA, and close to TOA/TDOA in some more informative areas. Road maps are the most informative, but only applicable to road-bound mobility.

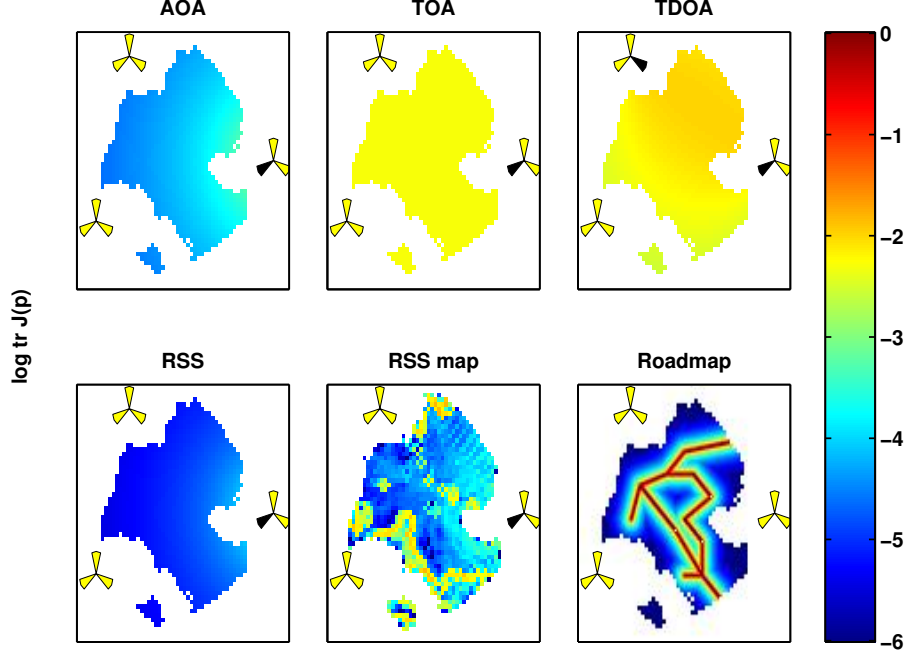


Fig. 4. Spatial distribution of the scalar measure $\log_{10} J_{\text{tr}}(p)$ related to the Fisher Information Matrix for some central measurements relative cell A (and cell B in case of TDOA) using the error standard deviation from Table 1.

The Cramer-Rao Lower Bound is given by

$$\text{Cov}(\hat{p}) = E(p^o - \hat{p})(p^o - \hat{p})^T \geq J^{-1}(p^o), \quad (5)$$

where p^o denotes the true position. The CRLB holds for any estimate of \hat{p}_t , in particular the ones based on minimizing the criteria in the previous sub-section. The general Cramer-Rao theory states that the ML estimate asymptotically, when the number of static measurements increases, reaches this bound. For that reason, computing the right hand side of (5) often gives a good idea of how suitable a given sensor configuration is for positioning. It can also be used for *system design*, e.g. where to put the base stations or what information to include in the protocol standard.

In practice, the root mean square error (RMSE) is perhaps of more importance. This can be interpreted as the achieved position error in meters. The CRLB implies the following bound:

$$\text{RMSE} = \sqrt{(X^o - \hat{X})^2 + (Y^o - \hat{Y})^2} = \sqrt{\text{tr Cov}(\hat{p})} \geq \sqrt{\text{tr } J^{-1}(p^o)} \quad (6)$$

If RMSE requirements are specified, it is possible to include more and more measurements in the design until (6) indicates that the amount of information is enough.

The FCC requirements are expressed as confidence intervals for the position error, and one requirement on mobile-centric positioning is $\text{Prob}(|\hat{p} - p^o| < 50) = \text{Prob}(|\hat{p} - p^o|^2 < 50^2) < 67\%$. To express this in terms

of FIM, we assume a circular positioning error distribution. This means $J(p^o) = \kappa I$ and with an estimator that reaches the CRLB $\text{Cov}(\hat{p}) = \kappa^{-1}I$. Furthermore, assuming that the position estimate \hat{p} distribution is Gaussian yields

$$\kappa|\hat{p} - p^o|^2 = \kappa|\hat{X} - X^o|^2 + \kappa|\hat{Y} - Y^o|^2 \in \chi^2(2) = \exp(0.5). \quad (7)$$

This gives the following requirement for sufficient information κ a function of the confidence level 100β % and the specified positioning error δ in meters

$$\kappa \geq \frac{2}{\delta^2} \log \frac{1}{1 - \beta}. \quad (8)$$

For the two FCC requirements $(\beta, \delta) = (0.67, 50 \text{ m})$ and $(\beta, \delta) = (0.95, 150 \text{ m})$, this evaluates to $\kappa \geq 0.00089 = 10^{-3.1}$ and $\kappa \geq 0.00027 = 10^{-3.6}$. The former is thus the dominating requirement. In the general case with an elliptic position error distribution, κ should be compared to $J_{\min}(p)$ in (4) to ensure sufficient information. Figure illustrate the spatial distribution of $\log_{10} J_{\min}(p)$ for the different types of measurements (each case with a measurement triplet relative cells A, B and C). One conclusion is the TOA and TDOA are capable of meeting the requirements with these assumptions, while RSS is not. It is also obvious that the RSS map increases the information in the RSS measurements partly due to less measurement noise, partly due to larger variations in $h(p)$. AOA may meet the requirements. The information can be further increased e.g. by using more measurements or using a digital road map for automotive applications.

Example 3 *The RMSE lower bounds from (6) for the TOA and TDOA measurements in Example 1 are plotted in Figure 6. The level curves are scaled by σ_e , so a range error with standard deviation of 100 meter will in the most favorable position lead to a position estimation error of 100 meter. A bit counter-intuitive, TDOA and TOA give the same performance close to the origin. To explain this, note that if all signals arrive simultaneously to all receivers, the transmission time does not add any information.*

3.3. Position Estimation

The two most well known and useful search methods for non-linear optimization are summarized in Table 3. Example 4 below illustrates typical performances. For further illustrations on computing the ML estimate for TDOA measurements, see [25, 26].

Example 4 *Consider again the TDOA estimation problem in Example 1. The least squares loss functions in Figure 2 reveals that the non-linear equations have no local minima, so both a gradient and a Newton-Raphson algorithm should converge from any initial point. Figure 7 shows examples of so called learning curves, illustrating how the*

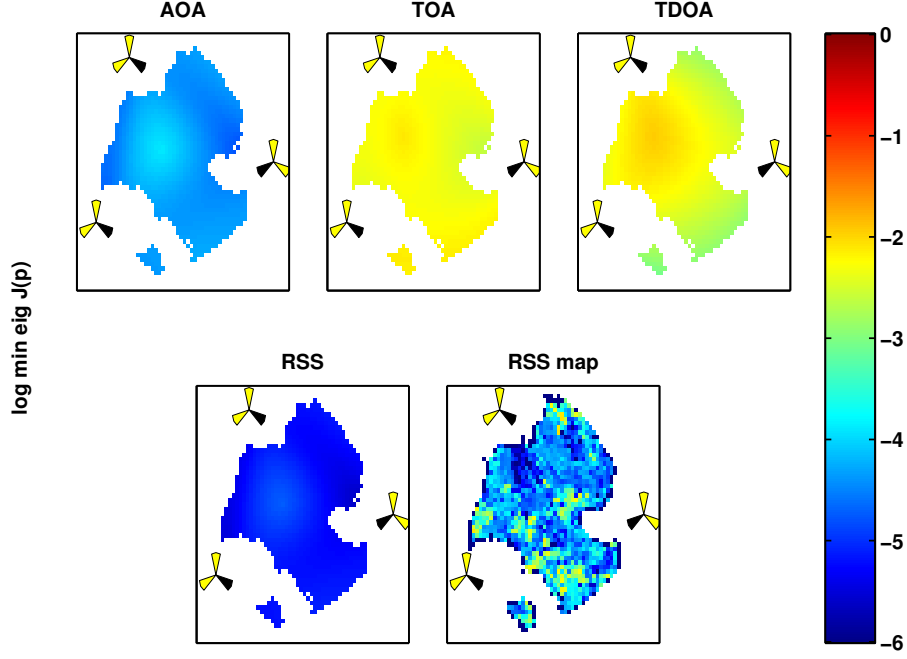


Fig. 5. Spatial distribution of the minimum Fisher Information Matrix eigenvalue $\log_{10} \min \text{eig } J(p)$ for measurements triplets relative cells A, B and C and noise error standard deviations from Table 1.

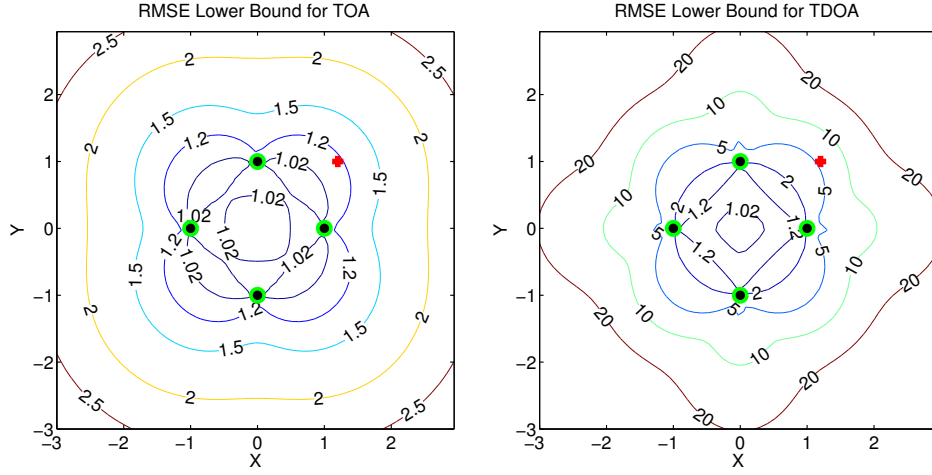


Fig. 6. Same scenario as in Figure 2. RMSE lower bound implied by the CRLB for TOA and TDOA, respectively, measurements. The unit is scaled to the measurement standard deviation.

Steepest descent	$\hat{p}_k = \hat{p}_{k-1} + \mu_k H^T(\hat{p}_{k-1})(y - H(\hat{p}_{k-1})\hat{p}_{k-1})$
Newton-Raphson	$\hat{p}_k = \hat{p}_{k-1} + \mu_k (H^T(\hat{p}_{k-1})R^{-1}H(\hat{p}_{k-1}))^{-1} H^T(\hat{p}_{k-1})R^{-1}(y - H(\hat{p}_{k-1})\hat{p}_{k-1})$

Table 3. Estimation algorithms applicable to the NLS and WNLS optimization criteria in Table 2.

initial position estimate at $(-1,2)$ improves with the iterations for both TOA and TDOA measurements. Note how slowly the steepest descent algorithm converges for TDOA measurements. For steepest descent $\mu_k = 0.25$, and for Newton-Raphson $\mu_k = 0.5$.

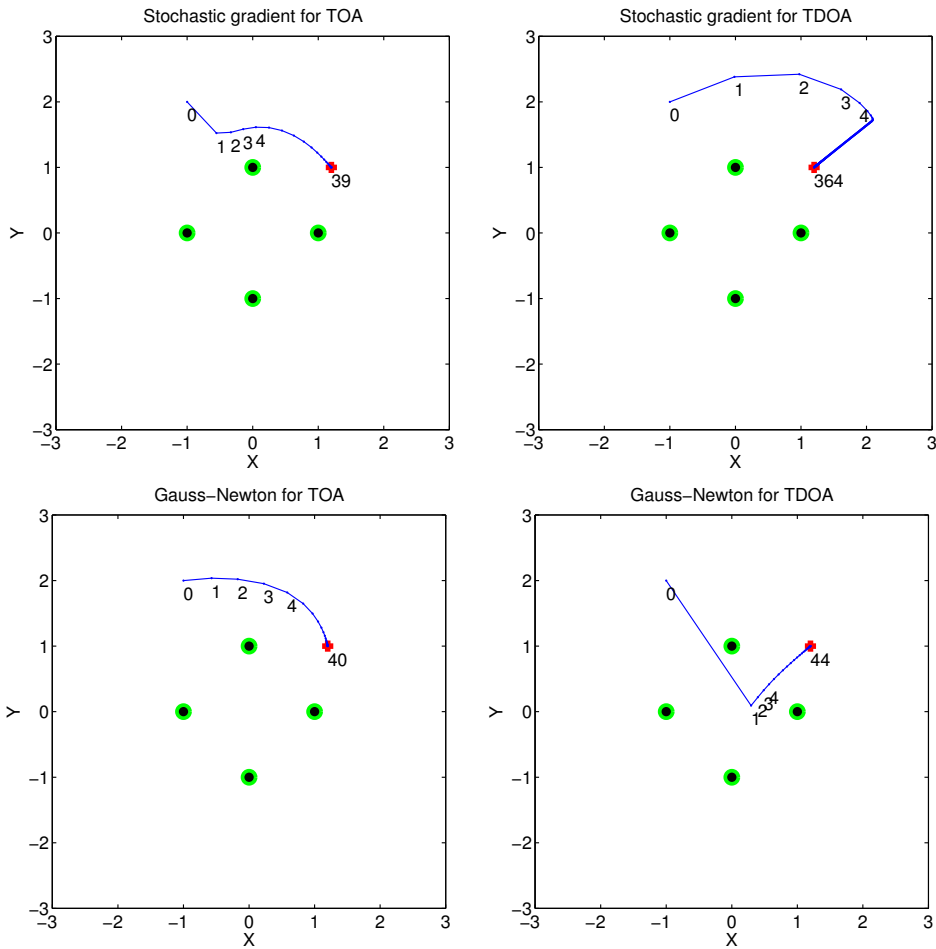


Fig. 7. Algorithms for minimizing the non-linear least squares criterion. First column: Steepest descent and Gauss-Newton algorithms for TOA measurements. Second column: Steepest descent and Gauss-Newton algorithms for TDOA measurements. The numbers indicate iteration index k in Table 3. Compare to the non-linear least squares loss functions in Figure 2.

3.4. Non-Line of Sight Problems

All measures suffer from the problem of non-line of sight, and the positioning becomes unreliable. This problem can be encountered in two ways:

- Use a robust error distribution. For instance, a TOA can have a long tail for positive errors.

- Include some logic in the search algorithm to rule out such outliers.

See [27, 28] for some algorithms in the second category. In the FIM context, it is evident that a non-line-of-sight measurement does not add significant information. The associated measurement error standard deviation σ_e is high assuming a Gaussian zero-mean error distribution, and the contributing information is proportional to σ_e^{-2} .

4. DYNAMIC CASE

4.1. Motion Models

The key idea with filtering is to include the terminal velocity in a dynamic model, so a prediction of the next position can be computed. Depending on the context, the actual two-dimensional mobile velocity v_t might be completely unknown, partly known (Doppler shift) or measurable (the natural example is a car-mounted system) or estimated in the model. The simplest possible motion models based on random walk, with or without velocity measurements, are summarized in Table 4. Any model suggested in the target tracking literature is plausible also for this application, see for instance the survey [29], but we focus on the simplest cases. Higher order models can decrease estimation error slightly, but will not drastically change our conclusions.

Random walk model:	$p_{t+1} = p_t + T_s w_t$
Velocity sensor model:	$p_{t+1} = p_t + T_s v_t + T_s w_t$
Random force model:	$\begin{pmatrix} p_{t+1} \\ v_{t+1} \end{pmatrix} = \underbrace{\begin{pmatrix} I & T_s \cdot I \\ 0 & I \end{pmatrix}}_F \begin{pmatrix} p_t \\ v_t \end{pmatrix} + \underbrace{\begin{pmatrix} T_s^2/2 \cdot I \\ T_s \cdot I \end{pmatrix}}_G w_t$
Inertial sensor model:	$\begin{pmatrix} p_{t+1} \\ v_{t+1} \end{pmatrix} = \begin{pmatrix} I & T_s \cdot I \\ 0 & I \end{pmatrix} \begin{pmatrix} p_t \\ v_t \end{pmatrix} + \begin{pmatrix} T_s^2/2 \cdot I \\ T_s \cdot I \end{pmatrix} a_t + \begin{pmatrix} T_s^2/2 \cdot I \\ T_s \cdot I \end{pmatrix} w_t$

Table 4. Examples of simple motion models, where T_s is the sample interval of the model, and w_t the process noise describing the mobility variations. Velocity and acceleration are denoted v_t and a_t , respectively.

The measurement equation is still on the form $y_t = h(p_t, p^i) + e_t$ as discussed in Section 2, with the corresponding measurement FIM $J(p_t^o)$. The filtering CRLB depends on $J(p_t^o)$, but also on the motion model selection and the user mobility assumptions. Due to averaging effects, the bound will decrease considerably compared to the static case. Another advantage with temporal data and filtering compared to estimation in the static case is that it is possible to handle an under-determined equation system in the measurement equations.

4.2. Fundamental Performance Bounds

Recently, location performance in the dynamic case in terms of the Cramer-Rao Lower Bound (CRLB) has been studied in [30, 31, 32] for the TDOA case. We here present a general derivation. The CRLB for non-linear filtering was derived in [33]. In short, they presented a recursion for non-linear models similar to the information filter version of the Riccati equation that computes a lower estimation bound P_t . The random walk model and velocity sensor model in Table 4 with process noise covariance matrix $\text{Cov}(w_t) = Q_t$ both result in the same recursion

$$\text{Cov}(p_t) \geq P_t, \quad (9)$$

$$P_{t+1} = ((P_t + Q_t)^{-1} + J(p_t^o))^{-1}. \quad (10)$$

In the cases with a velocity state in Table 4, define $H = (I, 0)$. This gives

$$\text{Cov}(p_t) \geq H P_t H^T, \quad (11)$$

$$P_{t+1} = ((F P_t F^T + G Q_t G^T)^{-1} + H^T J(p_t^o) H)^{-1}. \quad (12)$$

These expressions clearly show the compromise between mobility (Q) and information (J), and further down a few specific cases of special interest will be pointed out.

The position dependent information matrix $J(p^o)$ is under mild conditions on the measurement relation $h(x)$ a smooth function, and can be considered constant for movements in a small neighborhood of p^o . The recursion will then converge to a stationary point.

We will in the sequel analyze the first two cases in Table 4 in more detail. For (10), the stationary value is given by

$$\bar{P} = ((\bar{P} + Q)^{-1} + J(p^o))^{-1}, \quad (13)$$

which has the solution (see Appendix B)

$$\bar{P} = -\frac{1}{2}Q + J^{-1/2}(p^o) \left(J^{1/2}(p^o)(Q + \frac{1}{4}QJQ)J^{1/2}(p^o) \right)^{1/2} J^{-1/2}(p^o). \quad (14)$$

The following procedure thus yields the bound for any wireless positioning application:

1. select measurements from Table 1,
2. compute the Fisher Information Matrix using (2) and (3),
3. select a motion model from Table 4,
4. compute (14).

We can point out a couple of important special cases:

- For the case with large mobility uncertainty, $Q \rightarrow \infty$, and (13) gives $P_t = J^{-1}(p^o)$, which is the static case.
- For the case of symmetric movements in more than one dimension, we can assume that $Q = qI$. The measurement equation can also be assumed to be symmetric in the different dimensions (it can always be transformed to this form anyway), which means $J = \kappa I$. Then, the asymptotic CRLB according to (14) is

$$\bar{P} = \left(-\frac{q}{2} + \sqrt{\frac{q}{\kappa}} \left(1 + \frac{q\kappa}{4} \right)^{1/2} \right) I \quad (15)$$

For the case of limited movements and/or little information in each measurements, $q\kappa/4 \ll 1$, a Taylor expansion yields $\bar{P} \approx (-q/2 + \sqrt{q/\kappa})I$. The other extreme case of very large movements and/or very informative measurements, $q\kappa/4 \gg 1$, we get after Taylor expansion $\bar{P} \approx \kappa^{-1}I$, which again is the static case.

- For the special case of no movement at all $Q = 0$, the solution is found from (10) directly (assuming $P_0^{-1} = 0$) as

$$P_t = \frac{1}{t} J^{-1}(p^o). \quad (16)$$

4.3. Position Filtering

The simplest approach would be to use adaptive filters similar to the numerical search schemes in Table 3. An adaptive algorithm based on the steepest descent principle is the Least Mean Square (LMS) algorithm. Similarly, the Recursive Least Squares (RLS) algorithm is an adaptive version of a Gauss-Newton search. The tuning parameter μ or λ controls the amount of averaging and reflects our belief in user mobility.

The last two models in Table 4 require state estimation, and the natural first try is the extended Kalman filter (EKF), where measurement errors are assumed Gaussian, and the non-linear measurement equation $y_t = h(p_t) + e_t$ is linearized around the current position estimate. In case of quite non-linear measurement equation $h(p_t)$, or very non-linear error distribution, the position estimate using the EKF is far from the CRLB. The computer intensive particle filter (PF) [34, 35] has been proposed for high-performance positioning [9]. The advantage is that all currently available information described in Section 2 is easily incorporated, including power attenuation and street maps. Some examples are provided in [36].

LMS	$\hat{p}_t = \hat{p}_{t-1} + \mu H^T(\hat{p}_{t-1})(y_t - H(\hat{p}_{t-1})\hat{p}_{t-1})$
RLS	$\hat{p}_t = \hat{p}_{t-1} + P_t H^T(\hat{p}_{t-1})(y_t - H(\hat{p}_{t-1})\hat{p}_{t-1})$ $P_t = \frac{1}{\lambda} \left(P_{t-1} - P_{t-1} H^T(\hat{p}_{t-1}) (\lambda R_t + H(\hat{p}_{t-1}) P_{t-1} H^T(\hat{p}_{t-1}))^{-1} H(\hat{p}_{t-1}) P_{t-1} \right)$
EKF	$\hat{p}_t = \hat{p}_{t-1} + P_{t t-1} H^T(\hat{p}_{t-1})(y_t - H(\hat{p}_{t-1})\hat{p}_{t-1})$ $P_{t t} = P_{t t-1} - P_{t t-1} H^T(\hat{p}_{t-1}) (R_t + H(\hat{p}_{t-1}) P_{t t-1} H^T(\hat{p}_{t-1}))^{-1} H(\hat{p}_{t-1}) P_{t t-1}$ $P_{t+1 t} = F P_{t t} F^T + G Q_t G^T$
PF	Initialize N particles $p_0^i, i = 1, 2, \dots, N$. For each time t : 1. Likelihood computation $\pi^i = p_E(y_t - h(p_t^i))$. 2. Resample N particles with replacement according to likelihood weight π^i . 3. Diffusion step: randomize w^i from p_W and let $p_{t+1}^i = F p_t^i + G w^i$.

Table 5. Adaptive filters applicable to the dynamic motion models in Table 4. The Least Mean Square (LMS) and Recursive Least Squares (RLS) algorithms are applicable to the first two models in Table 4, while the Extended Kalman Filter (EKF) and Particle Filter (PF) apply to more general models.

Example 5 *The following one-dimensional positioning example illustrate the interplay of true and modeled motion. The random walk model in one dimension is given by*

$$p_{t+1} = p_t + w_t \quad (17)$$

$$y_t = p_t + e_t. \quad (18)$$

The example can be generalized to independent motions in two and three dimensions. We assume a GPS-like measurement with sampling frequency 1 Hz and with Gaussian error with standard deviation 10 m ($\sigma_e^2 = 10^2$). The true motion corresponds to the cases in Table 6. Note that without an explicit velocity state, the model states that a walking user may change velocity from 3 m/s forwards to 3 m/s backwards in 1 second. Now, the actual

Mobility	$\sqrt{q} = \text{std}(w_t)$ [m/s]
Indoor	0.3
Walking	3
Car	30

Table 6. Random walk motion parameter.

motion is not known, and the problem is to design one process noise covariance matrix $\text{Cov}(w_t) = Q = qI$ that gives good overall performance. Figure 8 shows the root mean square error (RMSE) in meters. The plot reveals

that it is safer to over-estimate mobility than to under-estimate it. The worst thing that can happen is that we come back to the static case, that is $RMSE = \sigma_e = 10$ m. On the other hand, if we knew that the transmitter is not moving faster than 0.3 m/s, than the RMSE can be as low as 2.5 m.

This example is linear and Gaussian, so the Kalman filter attains the CRLB in equation (15), which is also plotted in Figure 8 for comparison.

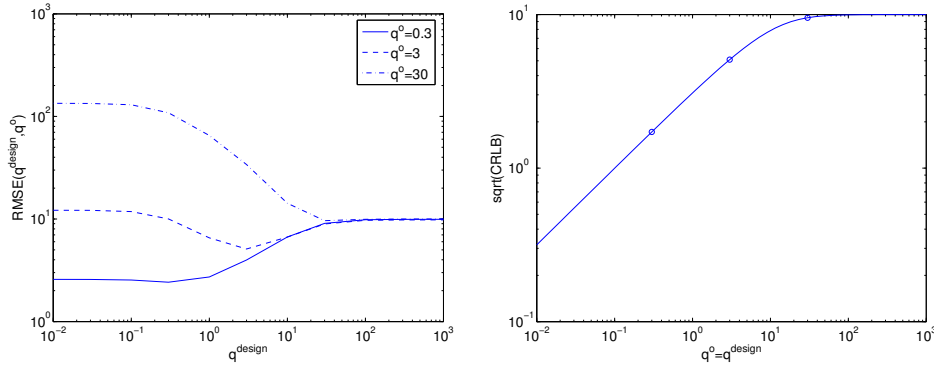


Fig. 8. Left: Resulting RMSE as a function of true transmitter mobility q^o and design parameter q^{design} . Right: The CRLB as a function of q^o , which in this case is attainable for the Kalman filter with $q^{design} = q^o$. The circles denote the three cases of q^o to the right.

The performance can be very much increased using the velocity sensors as accelerometers and gyroscopes. These are today available for cost and space-efficient mass production with fair accuracy.

Suppose first that it is possible to measure the velocity vector directly. This implies that the velocity sensor model in Table 4 is applicable, and the velocity measurement error becomes the random walk input w_t . This effectively means that we switch from one curve in the left plot of Figure 8 to another one below it, since we have a much smaller q^o , and the potential RMSE decreases according to the right plot in Figure 8. We can here read off the required velocity quality for a specified performance.

4.4. Filter Bank Techniques

There will be an increase in automotive telematic systems in the future, and related services will emerge. For that reason, the positioning system should try to detect whether the user is traveling by car. Similarly, walking and indoor users may be detected for increased performance. Introduce a motion state $m \in \mathcal{Z}$ for the cases indoor, walking and car (train) users similarly to Example 5.

In some cases the positioning system may know the motion state, for instance from the connection to an automotive docking station, or from the fact that the user is connected to an in-door base station. Otherwise, it is

plausible to use one adaptive filter from Table 5 with different models or with different values on motion parameter (see Table 6): Q for EKF and PF, step size for LMS or forgetting factor for RLS.

There are plenty of principles for how to combine the outputs of these filters to one position estimate, for instance using merging the states as in Interactive Multiple Models (IMM), pruning as in Adaptive Forgetting through Multiple Models (AFMM) or motion parameter estimation as in Hidden Markov Models (HMM), see [37] for an overview. A performance lower bound when the number of states increases is the CRLB to the right in Figure 8 as a function of true mobility.

5. CONCLUSIONS

Location in wireless networks is of increasing importance for safety, gaming and commercial services. There are plenty of measurements available today ranging from signal arrival times to maps over received power. We have here demonstrated how fundamental the Fisher Information Matrix for each measurement is to assess possible location performance. As one illustration, the FCC positioning requirements are transformed to requirements on sufficient information. Thereby, it is possible to investigate whether specific sensor configurations would provide acceptable accuracy. The information is additive, so several measurements increases information. The information concept can also handle and value less conventional measurements, such as digital propagation prediction maps and road maps. A further possibility to increase information, that may become necessary to achieve FCC requirements, is to use motion models and adaptive filters. This can increase the information by a factor of 10 for slowly moving users, when velocity or inertial sensors are used.

A practical question is whether there is an algorithm that attains the position error lower bound, and if this algorithm is possible to implement in practice. This of course depends from case to case, and we have briefly pointed out algorithms of particular interest with different complexity.

A. ANALYTICAL MEASUREMENT EQUATIONS

The most natural measurements in Table 1 can be expressed analytically. Table 7 summarizes expressions for $h(p_t, p_i)$ for RSS (Okumura-Hata model), TOA, TDOA and AOA.

Method	$h(p_t, p_i)$	$d h / d X$	$d h / d Y$
RSS:	$K + 10\alpha \log_{10} D_i$	$\frac{10\alpha}{\log 10} \frac{dx_i}{D_i^2}$	$\frac{10\alpha}{\log 10} \frac{dy_i}{D_i^2}$
TOA:	D_i	$\frac{dx_i}{D_i}$	$\frac{dy_i}{D_i}$
TDOA:	$D_i - D_j$	$\frac{dx_i}{D_i} - \frac{dx_j}{D_j}$	$\frac{dy_i}{D_i} - \frac{dy_j}{D_j}$
AOA¹:	$\alpha_i + \frac{180}{\pi} \arctan \frac{dy_i}{dx_i}$	$\frac{-dy_i}{D_i^2} \frac{180}{\pi}$	$\frac{dx_i}{D_i^2} \frac{180}{\pi}$

Table 7. Analytical expressions related to some measurements and gradients, where $dx_i = X - X_i$, $dy_i = Y - Y_i$, $D_i = \sqrt{dx_i^2 + dy_i^2}$ and analogous for dx_j , dy_j and D_j . 1) With sector antennas, it is not likely that directions are observed outside $\alpha_i \pm 90^\circ$, where α_i is the direction of the antenna main lobe.

B. STATIONARY RICCATI EQUATION FOR POSITIONING

The equation (13) can be rewritten first by removing the matrix inversions and then by completing the squares

$$\bar{P}^{-1} = (\bar{P} + Q)^{-1} + J(p^o) \quad (19a)$$

$$\Rightarrow \bar{P}J(p^o)\bar{P} + QJ(p^o)\bar{P} = Q \quad (19b)$$

$$\Rightarrow \left(\bar{P}J^{1/2}(p^o) + \frac{1}{2}QJ^{1/2}(p^o) \right) \left(J^{1/2}(p^o)\bar{P} + \frac{1}{2}J^{1/2}(p^o)Q \right) = Q + \frac{1}{4}QJQ \quad (19c)$$

$$\Rightarrow \left(J^{1/2}(p^o)\bar{P}J^{1/2}(p^o) + \frac{1}{2}J^{1/2}(p^o)QJ^{1/2}(p^o) \right) \left(J^{1/2}(p^o)\bar{P}J^{1/2}(p^o) + \frac{1}{2}J^{1/2}(p^o)QJ^{1/2}(p^o) \right) = J^{1/2}(p^o) \left(Q + \frac{1}{4}QJQ \right) J^{1/2}(p^o) \quad (19d)$$

$$\Rightarrow \bar{P} = -\frac{1}{2}Q + J^{-1/2}(p^o) \left(J^{1/2}(p^o)(Q + \frac{1}{4}QJQ)J^{1/2}(p^o) \right)^{1/2} J^{-1/2}(p^o) \quad (19e)$$

All involved matrices are symmetric, so it follows from (19b) that $QJ(p^o)\bar{P}$ is also symmetric, a fact used in the factorization (19c). The left and right multiplication with $J^{1/2}(p^o)$ in (19d) is done to get a symmetric solution for \bar{P} . We have found one symmetric positive semi-definite solution, and we know from the general Riccati theory that the solution is unique, hence we are done.

C. REFERENCES

- [1] J. J. Caffery and G. L. Stuber. Overview of radiolocation in CDMA cellular systems. *IEEE Communications Magazine*, 36(4), April 1998.
- [2] Y. Zhao. Standardization of mobile phone positioning for 3G systems. *IEEE Communications Magazine*, 40(7), July 2002.

- [3] C. Drane, M. Macnaughtan, and C. Scott. Positioning GSM telephones. *IEEE Communications Magazine*, 36(4), April 1998.
- [4] K. Pahlavan, L. Xinrong, and J.-P. Mäkelä. Indoor geolocation science and technology. *IEEE Communications Magazine*, 40(2), February 2002.
- [5] D. N. Hatfield. A report on technical and operational issues impacting the provision of wireless enhanced 911 services. Technical report, Federal Communications Commission, 2002.
- [6] Y. Zhao. Overview of 2G LCS technologies and standards. In *Proc. 3GPP TSG SA2 LCS Workshop*, London, UK, January 2001.
- [7] K. J. Krizman, T.E. Biedka, and T.S. Rappaport. Wireless position location: Fundamentals, implementation strategies, and sources of error. In *Proc. IEEE Vehicular Technology Conference*, June 1997.
- [8] Y.Okamura, E. Ohmori, T. Kawano, and K. Fukuda. Field strength and its variability in VHF and UHF land-mobile radio service. *Review of the Electrical Communication Laboratory*, 16(9-10), 1968.
- [9] F. Gustafsson, F. Gunnarsson, N. Bergman, U. Forssell, J. Jansson, R. Karlsson, and P-J. Nordlund. Particle filters for positioning, navigation and tracking. *IEEE Transactions on Signal Processing*, 50(2):425–437, February 2002.
- [10] R. Karlsson and F. Gustafsson. Particle filter and Cramer-Rao lower bound for underwater navigation. In *IEEE Conference on Acoustics, Speech and Signal Processing (ICASSP)*, Hongkong, China, Apr 2003.
- [11] B.T. Fang. Simple solutions for a hyperbolic and related position fixes. *IEEE Transactions on Aerospace and Electronic Systems*, 26(5), September 1990.
- [12] S.M. Kay. *Fundamentals of signal processing – estimation theory*. Prentice Hall, 1993.
- [13] C. Botteron, A. Host-Madsen, and M. Fattouche. Effects of system and environment parameters on the performance of network-based mobile station position estimators. *IEEE Transactions on Vehicular Technology*, 53(1), January 2004.
- [14] C. Botteron, A. Host-Madsen, and M. Fattouche. Cramer-Rao bounds for the estimation of multipath parameters and mobiles' positions in asynchronous DS-CDMA systems. *IEEE Transactions on Signal Processing*, 52(4), January 2004.
- [15] C. Botteron, M. Fattouche, and A. Host-Madsen. Statistical theory of the effects of radio location system design parameters on the position performance. In *Proc. IEEE Vehicular Technology Conference*, Vancouver, Canada, September 2002.
- [16] C. Botteron, A. Host-Madsen, and M. Fattouche. Cramer-Rao bound for location estimation of a mobile in asynchronous DS-CDMA systems. In *Proc. IEEE Conference on Acoustics, Speech and Signal Processing*, Salt Lake City, UT, USA, May 2001.
- [17] E. Ström and F. Malmsten. A maximum likelihood approach for estimating DS-CDMA multipath fading channels. *IEEE Journal on Selected Areas of Communications*, 18(1), January 2000.

- [18] H. Koorapaty. Cramer-Rao bounds for time of arrival estimation in cellular systems. In *Proc. IEEE Vehicular Technology Conference*, Milan, Italy, May 2004.
- [19] N. Patwari, A.O. Hero III, M. Perkins, N.S. Correal, and R.J. O'Dea. Relative location estimation in wireless sensor networks. *IEEE Transactions on Signal Processing*, 51(8), August 2003.
- [20] H. Koorapaty, H. Grubeck, and M. Cedervall. Effect of biased measurement errors on accuracy of position location methods. In *Proc. IEEE Global Telecommunications Conference*, Sydney, Australia, November 1998.
- [21] H. Koorapaty. Barankin bound for position estimation using received signal strength measurements. In *Proc. IEEE Vehicular Technology Conference*, Milan, Italy, May 2004.
- [22] Y. Qi and Hisashi Kobayashi. On relation among time delay and signal strength based geolocation methods. In *Proc. IEEE Global Telecommunications Conference*, San Francisco, CA, USA, December 2003.
- [23] Y. Qi and H. Kobayashi. On geolocation accuracy with prior information in non-line-of-sight environment. In *Proc. IEEE Vehicular Technology Conference*, Vancouver, Canada, September 2002.
- [24] Y. Qi and H. Kobayashi. Cramer-Rao lower bound for geolocation in non-line-of-sight environment. In *Proc. IEEE Conference on Acoustics, Speech and Signal Processing*, Orlando, FL, USA, May 2002.
- [25] A. Urruela and J. Riba. Novel closed-form ML position estimator for hyperbolic location. In *Proc. IEEE Conference on Acoustics, Speech and Signal Processing*, Montreal, Canada, May 2004.
- [26] F. Gustafsson and F. Gunnarsson. Positioning using time-difference of arrival measurements. In *IEEE Conference on Acoustics, Speech and Signal Processing (ICASSP)*, Hongkong, China, Apr 2003.
- [27] J. Riba and A. Urruela. A non-line-of-sight mitigation technique based on ML-detection. In *Proc. IEEE Conference on Acoustics, Speech and Signal Processing*, Montreal, Canada, May 2004.
- [28] J. Zhen and S. Zhang. Adaptive AR model based robust mobile location estimation approach in NLoS environment. In *Proc. IEEE Vehicular Technology Conference*, Milan, Italy, May 2004.
- [29] X.R. Li and V.P. Jilkov. Survey of maneuvering target tracking. part i: Dynamic models. *IEEE Transactions on Aerospace and Electronic Systems*, 39(4):1333–1364, 2003.
- [30] A. Urruela and J. Riba. A novel estimator and performance bound for time propagation and Doppler based radio-location. In *Proc. IEEE Conference on Acoustics, Speech and Signal Processing*, Hong Kong, P.R. China, April 2003.
- [31] A. Urruela and J. Riba. A novel estimator and theoretical limits for in-car radio-location. In *Proc. IEEE Vehicular Technology Conference*, Orlando, FL, USA, October 2003.
- [32] A. Urruela and J. Riba. Efficient mobile location from time measurements with unknown variances in dynamic scenarios. In *Proc. IEEE Workshop on Signal Processing Advances in Wireless Communications*, Lisboa, Portugal, July 2004.

- [33] N. Bergman. Posterior Cramér-Rao bounds for sequential estimation. In A. Doucet, N. de Freitas, and N. Gordon, editors, *Sequential Monte Carlo Methods in Practice*. Springer-Verlag, 2001.
- [34] N.J. Gordon, D.J. Salmond, and A.F.M. Smith. A novel approach to nonlinear/non-Gaussian Bayesian state estimation. In *IEE Proceedings on Radar and Signal Processing*, volume 140, pages 107–113, 1993.
- [35] A. Doucet, N. de Freitas, and N. Gordon, editors. *Sequential Monte Carlo Methods in Practice*. Springer Verlag, 2001.
- [36] P.-J. Nordlund, F. Gunnarsson, and F. Gustafsson. Particle filters for positioning in wireless networks (invited). In *Proceedings of European Signal Processing Conference (EUSIPCO)*, Toulouse, France, September 2002.
- [37] F. Gustafsson. *Adaptive filtering and change detection*. John Wiley & Sons, Ltd, 2000.